Hexagonal Ring Submicro- and Nanocrystals of a La–Hexacyanoferrate Coordination Polymer

Nobuyuki Kondo, Masato Kurihara,* Mami Yamada,† Mikio Miyake,† Masahiko Nishijima,††
Tetsu Ohsuna,†† Fujio Mizukami,††† and Masatomi Sakamoto
Department of Material and Biological Chemistry, Faculty of Science, Yamagata University, Kojirakawa-machi 1-4-12, Yamagata 990-8560
†*School of Materials Science, Advanced Institute of Science and Technology (JAIST), Asahidani 1-1, Tatsunokuchi-machi, Nomi-gun, Ishikawa 923-1292*
††*Institute for Materials Research, Tohoku University, Katahira 2-1-1, Aoba-ku, Miyagi 980-8577*
†††*Laboratory for Membrane Chemistry, National Institute of Advanced Industrial Science and Technology (AIST Tohoku), Nigatake 4-2-1, Miyagino-ku, Sendai 983-8551*

(Received February 1, 2005; CL-050145)

Hexagonal disk crystals of a La–hexacyanoferrate coordination polymer were obtained by reversed micelle technique. The {001} surface capping of the surfactants leads to the hexagonal disk shape evolution with the completely developed {001} surface. The hexagonal disks are changed into hexagonal rings through spontaneous and anisotropic surface etching along the [001] direction from both sides of the hexagonal disk.

Generally, the crystal shapes of metal and metal oxide nanoparticles can be controlled by interaction between the surrounding ions or molecules and the crystal surface.[1] Crystal surface energy, especially for the metal coordination compounds, is inherently fascinating, because of the diversity of the coordination structures and the crystal packing. Recently, the syntheses and physical properties of the Prussian blue analogue nanoparticles, $A_k[B(CN)_6]_l \cdot nH_2O$, such as Fe–CN–Co,[2–4] Cr–CN–Cr,[2] Cr–CN–Co,[4] Fe–CN–Ni,[3,5] Fe–CN–Fe,[6] and Co–CN–Eu[7] systems, have been intensively investigated, since the first report on preparation of the well-shaped Prussian blue nanocubes.[8] Nevertheless no other crystal shapes have been discovered except nanocubes[2,4,5] and nanospheres.[3,6,7] Herein, we show hexagonal disk submicro- and nanocrystals of a cyano-bridged La–hexacyanoferrate coordination polymer, and an anisotropic surface etching phenomenon to transform the hexagonal disk to a hexagonal ring, prepared by a reversed micelle reaction.

In preparing the submicro- and nanocrystals of a La–hexacyanoferrate, aqueous solutions (0.40 M) of $La(NO_3)_3$ and $K_3[Fe(CN)_6]$ were dispersed into 2.0 mL of a hexane solution (0.20 M) of AOT (sodium bis(2-ethylhexyl)sulfosuccinate). The two clear reversed micelle solutions were mixed to form the La–hexacyanoferrate nanocrystals. Figure 1a shows a transmission electron microscopy (TEM, JEOL JEM 2000EX II) image of the nanocrystals grown in the reversed micelle solution for 4 days after the coordination reaction was initiated by combining their reversed micelles. Hexagonal crystals appeared and the size distribution of the hexagons was from 30 to over several hundreds nm. The shape of the hexagonal crystals is a uniform hexagonal disk, as shown in a scanning electron microscopy (SEM, HITACHI FE SEM S-800) image of a population of the submicro crystals (Figure 1b). STEM (scanning transmission electron microscope)–EDX (energy dispersed X-ray analysis) (JEOL JEM-3000F) confirmed that the metal composition of the hexagonal disk crystals is Fe:La = 1:1. The La–hexacyanoferrate crystals were obtained as the hexagonal crystal system of

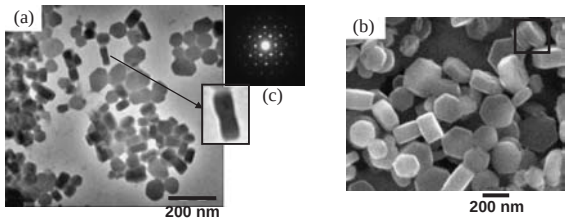

Figure 1. TEM (a) and SEM (b) images of the hexagonal disk submicro- and nanocrystals of $La[Fe(CN)_6]\cdot 5H_2O$ well-dispersed in the AOT/hexane, and the ED pattern (c). The dented crystals along the [001] direction are shown in the boxes.

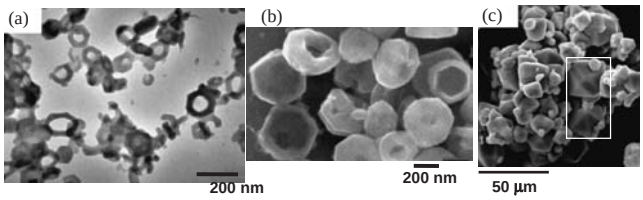

Figure 2. TEM (a) and SEM (b) images of a population of the hexagonal ring submicro- and nanocrystals, well-dispersed in the AOT/hexane and SEM image (c) of the bulk crystals of $La[Fe(CN)_6]\cdot 5H_2O$. The schematic representation of the bulk crystal in Scheme 1 corresponds to the crystal shape in the box.

$La[Fe(CN)_6]\cdot 5H_2O$ and the detailed X-ray crystallographic structure was already determined.[9] The electron diffraction (ED) pattern of the hexagonal disk crystal is in good agreement with simulation for the hexagonal plane, {001}, based on the X-ray crystallographic structure of $La[Fe(CN)_6]\cdot 5H_2O$. The lattice constant, a, of the hexagonal disk crystal is $\approx$7.5 Å calculated from the ED pattern (Figure 1c), which is consistent with $a = 7.541(3)$ Å of the bulk crystals, $La[Fe(CN)_6]\cdot 5H_2O$.[9] This fact reveals that the hexagonal disk crystals observed by the TEM and SEM images are an isostructural system with bulk crystals of $La[Fe(CN)_6]\cdot 5H_2O$.

Surprisingly, a large population of hexagonal ring nanocrystals was observed on the same TEM grid (Figure 2a). A dent along the six-fold axis on the {001} plane is confirmed from the shade in the side-view of the hexagonal disk crystals in the TEM, and in the SEM image (Figures 1a and 1b).

In $w = [H_2O]/[AOT] = 7$, the water droplet diameter of the reversed micelle is estimated to be 2–3 nm.[2] The initial com-

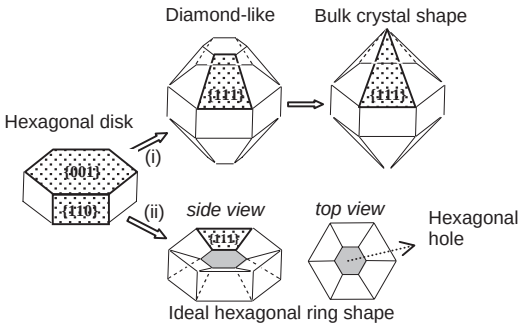

Scheme 1. Schematic representation of various crystal shapes of $La[Fe(CN)_6]\cdot 5H_2O$ and the crystal growth (i) and the surface etching (ii) pathways along the [001] direction.

bination of two water droplets containing La^{3+} and $[Fe(CN)_6]^{3-}$ produces a nanocluster consisting of 10–34 $La[Fe(CN)_6]$ components. It is understandable that the large hexagonal disk crystals of $La[Fe(CN)_6]\cdot 5H_2O$ are formed by aggregation of the nanoclusters. A similar crystal growth process has been speculated in the case of the Co–hexacyanoferrate nanocubes.[2] One hour after the initiation of the coordination reaction, hexagonal disk crystals ranging from 30 to 100 nm in size appeared; amorphous particles were also observed over a size distribution of 50 nm, which look like an aggregated shape of 10 nm-sized nanospheres according to the TEM image. However, similar hexagonal ring crystals were not observed in the reaction period. This suggests that the crystal growth takes place via the very rapid aggregation of the nanoclusters to form the hexagonal disk shape, and the hollow of the hexagonal disks is then gradually expanded during their long time exposure to the ionic surfactant, AOT.

The micrometer-sized bulk crystals of $La[Fe(CN)_6]\cdot 5H_2O$ immediately precipitated from an aqueous mixture of La^{3+} and $[Fe(CN)_6]^{3-}$ are composed of the highly developed {111} and {110} faces without the {001} plane (Figure 2c and Scheme 1). This crystal shape shows complete crystal growth in the [001] direction by accelerating the release of the component ions from the {001} plane (Scheme 1, pathway (i)). The La ions are located on the {001} plane and inside the {110} plane, according to the X-ray crystallographic analysis.[9] In the reversed micelle solution, a large excess amount of the AOT anion co-exists with the La^{3+} ions, and the molar ratio is AOT:La^{3+} = 20:1. When the La^{3+} ions on the {001} face are more effectively exposed to the surface interaction with the AOT anion through weak coordination, the release of La^{3+} ions from the {001} plane is decelerated. The {001} surface capping due to AOT resulted in the evolution of a hexagonal disk shape with a completely developed {001} surface.[1b] The moderate {001} face-developing leads to a diamond-like shape truncated along the [001] direction (Scheme 1), while the diamond-like crystals do not appear under these reaction conditions.

The hexagonal disk shape probably evolved through a kinetic crystal growth pathway including the very rapid aggregation of the nanoclusters, *vide supra*. On the other hand, many of the hexagonal disks are dented along the six-fold axis on the {001} plane (Figure 1), indicating the possibility of a slow release of La^{3+} on the {001} face, that is an anisotropic crystal etching from the kinetically grown hexagonal disk crystal. The capping of AOT anions on the {001} is still incomplete, because the coordination bond between the sulfonic moiety and the surface La^{3+} ions is very weak. This is the cause of the slow release of the La^{3+} ions. The metal composition is estimated to be Fe:La = 1:0.8 near the hexagonal center and Fe:La = 1:1 near the hexagonal edge of the dented crystal, based on the detailed STEM–EDX study. From this result, we deduce that the preceding release of La^{3+} from the {001} surface occurs near the hexagonal center and the $[Fe(CN)_6]^{3-}$ components are still attached on the crystal surface. After the release of La^{3+}, the broken network structure on the surface results in further release of $[Fe(CN)_6]^{3-}$ during the formation of the hollow.

If the release rate from the {001} plane dominates the restorable crystal growth rate of the {001} plane, the hexagonal ring crystals can be generated through an ideal anisotropic etching pathway from both the {001} sides of the hexagonal disk, showing decrease in the {001} area, and increase in the {111} area (Scheme 1, pathway (ii)). In the relatively smaller hexagonal crystals, a clearer hole appears around the center of the hexagon (Figure 2a), while some of the larger crystals are irregularly holed (Figure 2b). The hole shape is an incomplete hexagon, which may be due to weak facets of the {111} and {001} planes.

We found a new crystal shape in the Prussian blue analogue nanoparticles, "hexagonal ring", led by spontaneous and anisotropic surface etching depending on the interaction between the surface La^{3+} and the anionic surfactant. Comparison of each crystal face between the hexagonal disk and the ring is under further investigation by means of ED and XRD analyses.

This work was supported by Grant-in-Aid for Scientific Research (Nos. 15750044 and 16710069) and "Nanotechnology Supports Project" of the Ministry of Education, Culture, Sports, Science and Technology, Japan, and the Kurata Hitachi Fundation.

References

1 a) R. L. Penn and J. F. Banfield, *Geochim. Cosmochim. Acta*, **63**, 1549 (1999). b) J. Cheon, N.-J. Kang, S.-M. Lee, J.-H. Lee, J.-H. Yoon, and S. J. Oh, *J. Am. Chem. Soc.*, **126**, 1950 (2004). c) F. Li, Y. Ding, P. Gao, X. Xin, and Z. L. Wang, *Angew. Chem., Int. Ed.*, **43**, 5238 (2004). d) G. S. Métraux, Y. C. Cao, R. Jin, and C. A. Mirkin, *Nano Lett.*, **3**, 519 (2003).
2 a) S. Vaucher, J. Fielden, M. Li, E. Dujardin, and S. Mann, *Nano Lett.*, **2**, 225 (2002). b) E. Dujardin and S. Mann, *Adv. Mater.*, **16**, 1125 (2004).
3 a) P. Y. Chow, J. Ding, X. Z. Wang, C. H. Chew, and L. M. Gan, *Phys. Status Solidi*, **180**, 547 (2000). b) C. W. Ng, J. Ding, P. Y. Chow, L. M. Gan, and C. H. Quek, *J. Appl. Phys.*, **87**, 6049 (2000).
4 M. Yamada, M. Arai, M. Kurihara, M. Sakamoto, and M. Miyake, *J. Am. Chem. Soc.*, **126**, 9482 (2004).
5 N. Bagkar, R. Ganguly, S. Choudhury, P. A. Hassan, S. Sawant, and J. V. Yakhmi, *J. Mater. Chem.*, **14**, 1430 (2004).
6 a) T. Uemura and S. Kitagawa, *J. Am. Chem. Soc.*, **125**, 7814 (2003). b) J. M. Domínguez-Vera and E. Colacio, *Inorg. Chem.*, **42**, 6983 (2003). c) T. Uemura, M. Ohba, and S. Kitagawa, *Inorg. Chem.*, **43**, 7339 (2004). d) Z. Li, J. Zhang, T. Mu, J. Du, Z. Liu, B. Han, and J. Chen, *Colloids Surf., A*, **243**, 63 (2004).
7 N. Kondo, A. Yokoyama, M. Kurihara, M. Sakamoto, M. Yamada, M. Miyake, T. Ohsuna, H. Aono, and Y. Sadaoka, *Chem. Lett.*, **33**, 1182 (2004).
8 S. Vaucher, M. Li, and S. Mann, *Angew. Chem., Int. Ed.*, **39**, 1793 (2000).
9 W. E. Bailey, R. J. Williams, and W. O. Milligan, *Acta Crystallogr.*, **B29**, 1365 (1973).

Published on the web (Advance View) March 19, 2005; DOI 10.1246/cl.2005.590